Photon cascade emission in $SrAlF_5:Pr^{3+}$

2002 J. Phys.: Condens. Matter 14 8889

(http://iopscience.iop.org/0953-8984/14/38/312)

INSTITUTE OF PHYSICS PUBLISHING JOURNAL OF PHYSICS: CONDENSED MATTER

J. Phys.: Condens. Matter **14** (2002) 8889–8899 PII: S0953-8984(02)39305-6

Photon cascade emission in $SrAlF_5:Pr^{3+}$

A P Vink[1], P Dorenbos[1,5], J T M de Haas[1], H Donker[2], P A Rodnyi[3], A G Avanesov[4] and C W E van Eijk[1]

[1] Interfaculty Reactor Institute, Delft University of Technology, Mekelweg 15, 2629 JB Delft, The Netherlands
[2] Faculty of Applied Sciences, Delft University of Technology, Julianalaan 136, 2628 BL Delft, The Netherlands
[3] St Petersburg State Technical University, Polytekhnicheskaya 29, 195251 St Petersburg, Russia
[4] Kuban State University, Stavropolskaya 149, 350040 Krasnodar, Russia

Received 10 July 2002
Published 12 September 2002
Online at stacks.iop.org/JPhysCM/14/8889

Abstract

The optical properties of $SrAlF_5:Pr^{3+}$ are studied. Emission measurements up to 1200 nm under blue-light excitation in the $^3P_2$ level reveal a large number of emissions all originating from the $^3P_0$ level and the $^1D_2$ level. Under vacuum ultraviolet excitation in the $4f^15d^1$ bands, emission from the $^1S_0$ level, followed by emission from the $^3P_0$ level and the $^1D_2$ level takes place. This is known as the photon cascade emission process. The excitation spectrum of the $^1S_0$ emission was measured and was compared with the excitation spectrum of $SrAlF_5:Ce^{3+}$. The spectrum for $SrAlF_5:Pr^{3+}$ compared to $SrAlF_5:Ce^{3+}$ is at about 12 240 cm^{-1} higher energy. A study of the x-ray-excited emission in the temperature region from 100 to 350 K was performed, determining the processes responsible for both $^1S_0$ and $^3P_0/^1D_2$ emissions.

1. Introduction

The photon cascade emission (PCE) process was discovered independently by Piper [1] and Sommerdijk [2] in 1974 for $YF_3:Pr^{3+}$. In this process, excitation in the $4f^15d^1$ bands or directly in the $4f^2[^1S_0]$ level gives a two-step emission to the ground state: $^1S_0 \rightarrow {}^1I_6$ and $^3P_0 \rightarrow {}^3H_4$. The energy level scheme, showing quantum cutting, is depicted in figure 1. The PCE process is also know as quantum cutting or quantum splitting.

Quantum cutting phosphors are interesting for application in new xenon-based fluorescent lighting and flat-panel television screens (PDPs). The Pr^{3+} ion is not the only ion which can show quantum cutting. Wegh *et al* showed quantum cutting in $LiGdF_4$ doped with Eu^{3+} [3], and with both Er^{3+} and Tb^{3+} [4]. The Pr^{3+} ion shows quantum cutting in a large number of hosts, such as fluorides [5–9] and oxides [10–16]. However, not all hosts show quantum cutting (when doped with Pr^{3+}). For example, in the host $LiYF_4$, no $4f^2 \rightarrow 4f^2$ emission but

[5] Author to whom any correspondence should be addressed.

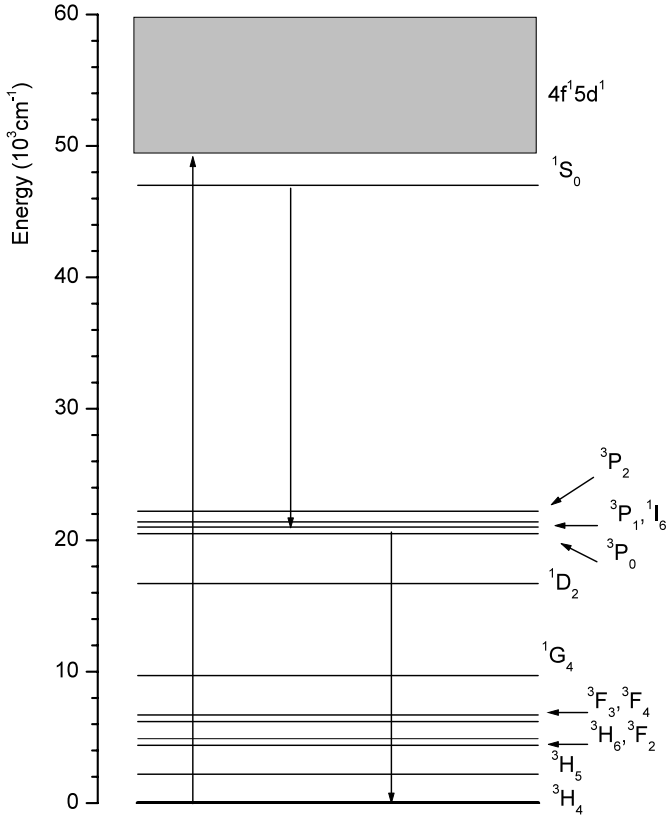

Figure 1. The energy level scheme of Pr^{3+} showing a two-step emission ($^1S_0 \rightarrow {}^1I_6$ and $^3P_0 \rightarrow {}^3H_4$) after excitation in the $4f^15d^1$ bands. The non-radiative emission steps: $4f^15d^1(1) \rightarrow {}^1S_0$ and $^1I_6 \rightarrow {}^3P_0$ are not shown.

$4f^15d^1 \rightarrow 4f^2$ emission is observed, as the $4f^15d^1$ bands are at lower energy than the $^1S_0$ $4f^2$ level [1].

The crystal structure of $SrAlF_5$ was described in [17]. Four different Sr sites are present with fluorine coordination from ten to twelve. When doped with Pr^{3+}, this ion resides on the divalent Sr site and not on the sixfold-coordinated Al site. In principle, site-selective excitation could resolve the different sites, but as there is not much difference in coordination between the different sites, excitation bands belonging to different sites overlap strongly. In this paper we focus on the results under excitation in the $^3P_2$ levels, in the $4f^15d^1$ bands and in the conduction band and we did not put effort into measuring the excitation and emission spectra of different sites separately.

The introduction of the trivalent Pr ion on the divalent Sr site requires charge compensation. No co-dopant, such as Na^+, was added. This absence of a co-dopant will probably not influence the spectroscopic properties, but just lower the amount of Pr^{3+} built in.

This paper first describes the optical properties of $SrAlF_5$:Pr^{3+}, starting by describing the emission in the visible and infrared spectral regions under excitation in the $^3P_2$ level. Furthermore, results on the quantum cutting behaviour will be described and the $4f^15d^1$ excitation spectrum is presented. The excitation spectrum of the $4f^15d^1$ bands was compared with the excitation spectrum of $SrAlF_5$:Ce^{3+} from [18].

The emission spectrum of $SrAlF_5:Pr^{3+}$ under x-ray excitation, measured at room temperature, was already published in [19]. This emission spectrum showed, besides broad-band emission, a large number of $4f^2 \rightarrow 4f^2$ emissions, all originating from the $^1S_0$, $^3P_0$ and $^1D_2$ levels. We present a study to investigate the intensity behaviour of these emissions at different temperatures (100–350 K). From the literature, two other Pr^{3+}-doped quantum cutting hosts under x-ray excitation are known. In [20] the emission properties of $YF_3:Pr^{3+}$ under x-ray excitation were reported, whereas the $LaF_3:Pr^{3+}$ material was studied both under optical and x-ray excitation in [21].

2. Experiments

2.1. Sample preparation

The $SrAlF_5:Pr^{3+}$ sample was synthesized in the Laser Materials Laboratory of the Kuban State University using standard procedures. The samples were prepared by firing stoichiometric mixtures of SrO, Al_2O_3 and Pr_6O_{11} at 800–1000 °C under a constant flow of twice-distilled HF. The Pr^{3+} concentration in the melt was 0.3 mol%. The incorporated Pr^{3+} concentration is probably lower. The sample was checked by means of x-ray diffraction and proved to be of single phase.

2.2. Measurements

Measurements for $SrAlF_5:Pr^{3+}$ at room temperature were performed on two different set-ups. Excitation spectra in the blue region and emission spectra up to 750 nm were measured using a Photon Technology International spectrofluorometer set-up equipped with a high-power xenon lamp and double-beam excitation and emission monochromator.

The emission spectrum up to 1200 nm was measured with another set-up. The excitation source was an optical parametric oscillator (Spectra Physics Quanta-Ray MOPO-710) pumped by the third harmonic ($\lambda_{exc} = 355$ nm) of a pulsed Nd:YAG laser (Spectra Physics Quanta-Ray GCR 170). The power density of the laser beam was attenuated with neutral density filters. The luminescence was detected with a liquid-nitrogen-cooled CCD camera (Princeton Instruments LN/CCD-1100PB), coupled to a Spex 340E monochromator, equipped with a 100 grooves mm^{-1} grating, blazed at 500 nm. The luminescence signal was focused on a round-slit multi-mode optical fibre bundle, whereas the output of this fibre was focused on the entrance slit of the monochromator using a Princeton Instruments Optical Fiber Adapter. The typical spectral resolution of this set-up is about 1.5 nm. Neither the excitation nor the emission spectra were corrected for the response of the system.

The low-temperature measurements of Pr^{3+} in $SrAlF_5$ were performed on the Deutsches Electronen Synchotron (DESY) in Hamburg using the SUPERLUMI set-up at HASYLAB. Details of the excitation set-up can be found elsewhere [22]. Excitation spectra were recorded in the region from 60–300 nm with a typical resolution of 0.3 nm. The light was detected using a solar-blind PMT (150–300 nm) or cooled PMT (200–600 nm), with resolutions of about 1 nm.

Measurements on the x-ray excitation set-up were performed using a Cu Kα x-ray source and an ARC VM502 monochromator, with a typical resolution of 2 nm. The light from the samples was detected using a Hamamatsu Photomultiplier. All x-ray-excited emission spectra were corrected for the response of the monochromator and the PMT.

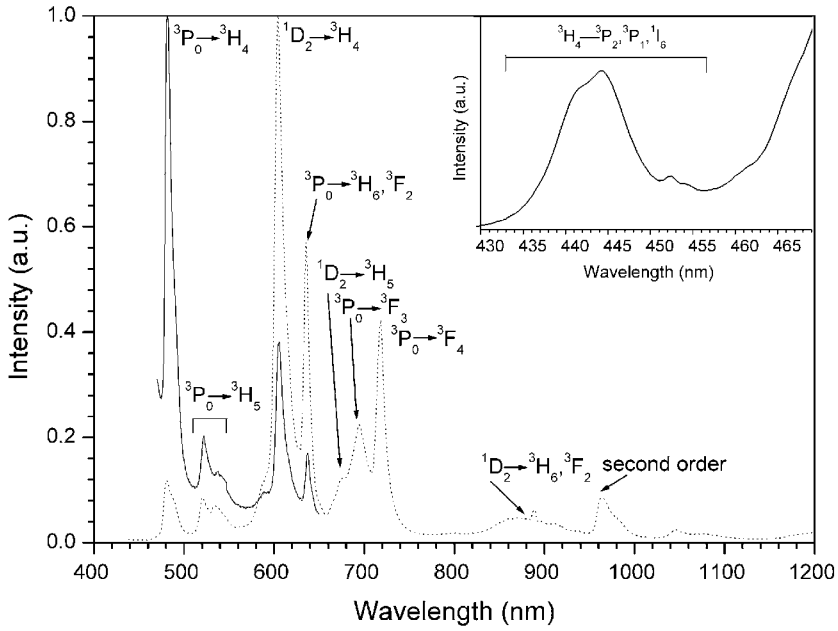

Figure 2. Emission spectra of $SrAlF_5:Pr^{3+}$ under excitation in the $^3P_2$ level ($\lambda_{exc} = 444$ nm, $T = 298$ K). The solid curve shows the emission measured with a PMT, whereas the dotted curve shows the emission measured with a CCD camera. Neither emission spectrum was corrected for the response of the system. The inset shows the excitation spectrum monitoring the $^3P_0 \rightarrow {}^3H_4$ emission at $\lambda_{em} = 481$ nm.

3. Results and discussion

3.1. Optical excitation

Two emission spectra under excitation in the $^3P_2$ level at 444 nm and measured at room temperature are shown in figure 2. The spectrum measured with a PMT (solid curve) shows strong $^3P_0$ emission and weak $^1D_2$ emission. The presence of more intense $^3P_0$ emission compared to that for $^1D_2$ can be ascribed to the low phonon energy in the fluoride host, resulting in a low transition probability for the non-radiative relaxation from the $^3P_0$ to the $^1D_2$ level. The emission spectrum, measured with a CCD camera (dotted curve), has a low intensity in the green spectral region, because of the low detection efficiency. No attempt was made to correct for the differences in sensitivity between the set-ups.

The inset in figure 2 shows the excitation spectrum corresponding to the $^3P_0 \rightarrow {}^3H_4$ emission. The lines belonging to $^3H_4 \rightarrow {}^3P_J (J = 0, 1, 2)$, $^1I_6$ transitions are not resolved. This is probably because of the existence of several sites in the $SrAlF_5$ host.

In the vacuum ultraviolet spectral region the $4f^15d^1$ bands can be excited. The Pr^{3+} $4f^15d^1$ excitation spectrum ($\lambda_{em} = 404$ nm) is shown in figure 3(A). The separate bands cannot be resolved in the excitation spectrum. This band probably consists of $4f^15d^1$ excitations of Pr^{3+} on multiple sites. The $4f^15d^1$ excitation spectrum of Pr^{3+} usually shows a $5d^1$ level splitting quite similar to that for Ce^{3+} and in addition some sub-structure. This sub-structure is ascribed to spin–orbit and electrostatic interactions between the $4f^1$ and $5d^1$ electrons [23]. As the Ce^{3+} ion in the excited state has no electron left in the $4f^n$ shell, both of these interactions are absent. However, even the five-band structure for the Ce^{3+} $4f^05d^1$ excitation spectrum from [18] is not

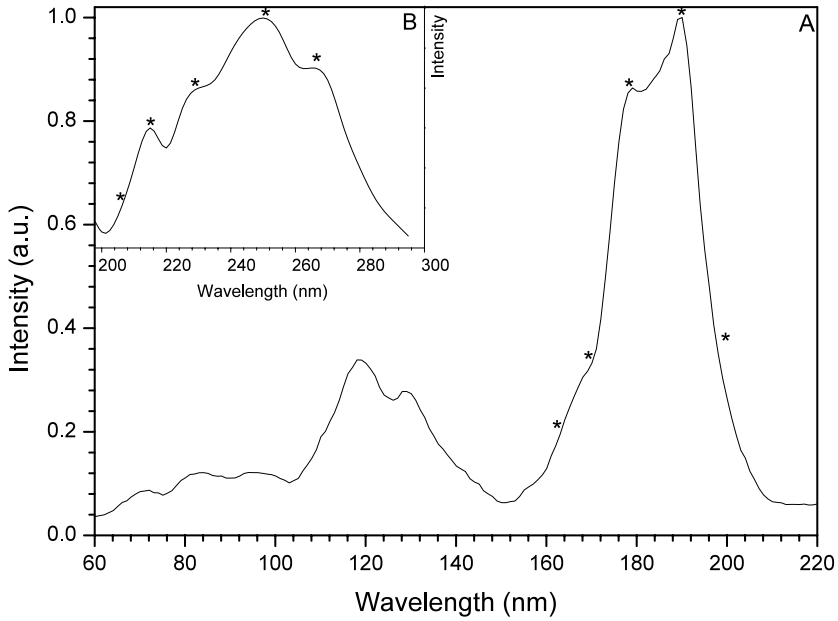

Figure 3. The excitation spectrum ($\lambda_{em} = 404$ nm, $T = 10$ K) of $SrAlF_5:Pr^{3+}$ showing the $4f^15d^1$ bands marked with asterisks. The inset shows an absorption spectrum of $SrAlF_5:Ce^{3+}$ taken from [18]. These five bands are also marked with asterisks.

well resolved; see figure 3(B) (inset). We have tentatively assigned the five bands for Ce^{3+} and marked these as five stars in figure 3(B). Adding 12 240 cm^{-1} to the energy of these bands, one obtains the positions of the corresponding bands for Pr^{3+} in figure 3(A). There is a reasonable agreement between the $4f^{n-1}5d^1$ structures for Ce^{3+} and Pr^{3+}. It must however be noted that there is more than one site present in $SrAlF_5$. Still, we can state that the energy difference between the $4f^15d^1$ band for $SrAlF_5:Pr^{3+}$ and $SrAlF_5:Ce^{3+}$ is about $12\,240 \pm 750$ cm^{-1}. This value is called ΔE(Ce, Pr) in [24, 25].

In figure 4, two emission spectra measured at $T = 10$ K can be observed. The solid curve shows the emission spectrum excited in the $4f^15d^1$ bands ($\lambda_{exc} = 190$ nm), whereas the dotted curve shows the emission spectrum when excited at 111 nm. Excitation with VUV radiation at 111 nm results in excitation into the conduction band of the material. In the emission spectrum a broad band around 360 nm can be observed, which can be assigned to emission from a localized electron–hole pair, a self-trapped exciton (STE). Besides the band emission, only weak $^3P_0 \rightarrow {}^3H_4$ emission can be observed.

In the emission spectrum measured under excitation directly in the $4f^15d^1$ bands, a large number of Pr^{3+} $4f^2$ emissions can be observed, including emissions from the $^1S_0$ level in the ultraviolet (UV) spectral region. As no $4f^15d^1 \rightarrow 4f^2$ emission was found, it must be concluded that the $4f^15d^1$ bands are at higher energy than the $^1S_0$ level for Pr^{3+} in all sites. All emissions, especially the $^1S_0 \rightarrow {}^1I_6$, are broad (about 1000 cm^{-1}), which could indicate that the emission line consists of a number of $^1S_0 \rightarrow {}^1I_6$ emissions from different sites.

3.2. X-ray excitation

In figure 5, emission spectra under x-ray excitation of $SrAlF_5:Pr^{3+}$ at $T = 100$ and 350 K are shown. A substantial difference between these emission spectra can be observed. In the 100 K

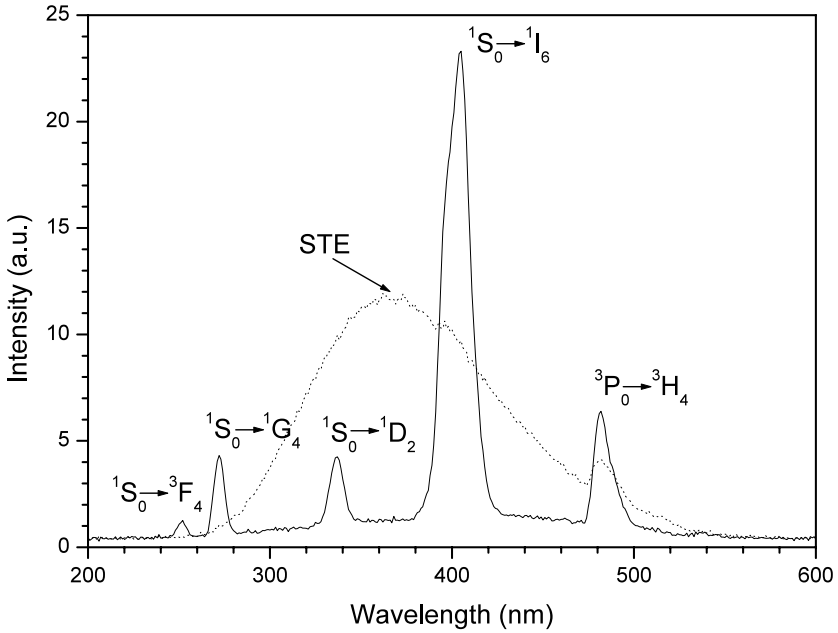

Figure 4. VUV-excited emission spectra of $SrAlF_5:Pr^{3+}$ measured at $T = 10$ K. The solid spectrum ($\lambda_{exc} = 190$ nm) shows the PCE process, whereas the dotted spectrum ($\lambda_{exc} = 111$ nm) shows the typical STE band around 360 nm.

spectrum a broad band is present which has a lower intensity at 350 K. This emission band originates from a STE and can also be found under optical excitation (see figure 4). Another feature is the observation of the PCE process at 350 K. No emission from the $^1S_0$ level is visible at 100 K.

The properties of the STE at different temperatures have been investigated for Ce^{3+}-doped materials [26]. In low-concentration Ce^{3+}-doped hosts, energy transfer from the STE to Ce^{3+} was described by a site-to-site hopping process. The probability of energy transfer to Ce^{3+} is increased at elevated temperatures as the mobility of an STE increases. At higher concentrations, another process becomes dominant. This process is recombination of the electron and the hole without formation of a STE. It was found for Ce^{3+} that this process is independent of temperature. For Ce^{3+}-doped materials, both processes eventually result in the same $4f^05d^1 \rightarrow {}^2F_{5/2}, {}^2F_{7/2}$ emission, and time-resolved measurements at different temperatures and concentrations have to be done to discriminate between the two processes.

The energy transfer from the STE to the impurity can also be observed for Pr^{3+}-doped materials. This process is, like for Ce^{3+}-doped materials, temperature dependent. To reach the $4f^15d^1$ bands or the $^1S_0$ level, the minimal energy for the STE must be 47 000 cm^{-1} (corresponding to a 215 nm transition). From figures 4 and 5, it can be observed that the energy of the STE is too small to excite either the $4f^15d^1$ states or the $^1S_0$ level of Pr^{3+}.

The shape and wavelength region of the STE band are typical for fluoride materials. Therefore, it is unlikely that the STE in $YF_3:Pr^{3+}$ is responsible, as was stated in [20], for the observation of the PCE process. The energy of the STE is however high enough to excite the $^3P_J (J = 0, 1, 2)$, $^1I_6$ levels of Pr^{3+}. The STE emission hardly shows any overlap with the $^1D_2$ level (see figure 5), but this level is fed by non-radiative relaxation from the $^3P_0$ level. So, energy transfer from the STE to the Pr^{3+} ion results in $^3P_0$ and $^1D_2$ emissions.

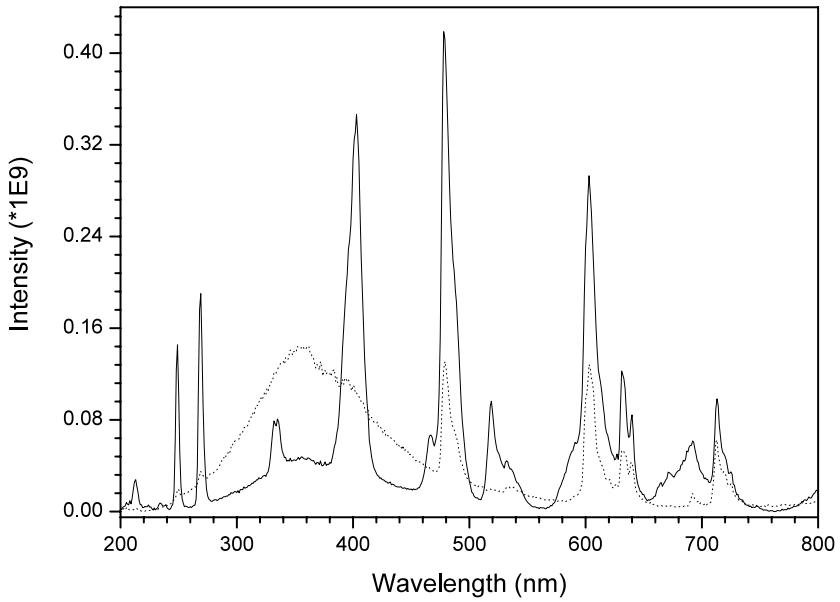

Figure 5. X-ray-excited emission spectra of $SrAlF_5:Pr^{3+}$ measured at $T = 100$ K (dotted curve) and $T = 350$ K (solid curve).

The process which results in quantum cutting is the recombination of the electron and the hole on the Pr^{3+} ion without formation of a STE. The same process is dominant for highly concentrated Ce^{3+}-doped scintillators and results in fast $4f^05d^1 \rightarrow {}^2F_{5/2}, {}^2F_{7/2}$ emission [26].

In figure 6 the intensity of the STE and three $4f^2 \rightarrow 4f^2$ emissions ($^1S_0 \rightarrow {}^1I_6$, $^3P_0 \rightarrow {}^3H_4$ and $^1D_2 \rightarrow {}^3H_4$) as a function of temperature is shown. The $^1S_0$ emission is absent at temperatures lower than 150 K, but increases rapidly at higher temperatures. Also the intensity of the $^3P_0$ and $^1D_2$ emissions increases at higher temperatures. The $^3P_0$ emissions gain intensity from transferred energy from the STE band and from the PCE process (second step). The emission from the $^1D_2$ level is excited via relaxation from the $^3P_0$ level.

The intensity difference between $^1S_0$ and $^3P_0$ remains constant up to about $T = 325$ K. At higher temperatures the increase of the $^1S_0$ emission becomes less steep. The $^3P_0$ emission still increases at the same rate because of the energy transfer from the STE to the Pr^{3+} ion. The $^1D_2$ emissions start to quench at much lower temperatures (from $T = 200$ K). This emission probably quenches through cross-relaxation of Pr^{3+} pairs [27].

The temperature dependence of the $^1S_0$ emission under x-ray excitation is quite striking, as for Ce^{3+}-doped hosts it was found that the process of electron–hole recombination (without intermediate STE formation) is temperature independent [26]. We envisage that some of the free electrons and holes are trapped at low temperatures. De-trapping at temperatures above 150 K then leads to $^1S_0$ emission.

Two possible explanations for the temperature dependence of the recombination process are proposed:

(1) The electron can recombine with Pr^{3+} forming Pr^{2+} and the hole can be trapped in a hole trap, e.g. a V_K centre.
(2) The hole recombines with Pr^{3+} to form Pr^{4+} and the electron is trapped in for example an anion vacancy, forming an F centre.

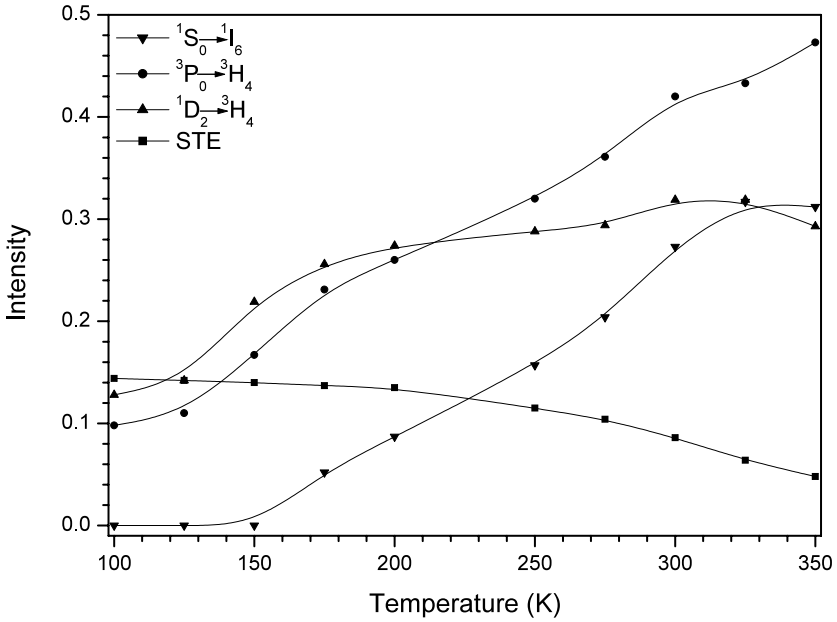

Figure 6. The intensity behaviour of the STE emission and three Pr^{3+} $4f^2$ emission curves at different temperatures for excitation with x-rays. The curves are drawn as a guide to the eye.

The hole (process 1) and the electron (process 2) can be de-trapped at elevated temperature and recombine at Pr^{4+} and Pr^{2+} resulting in population of the $4f^15d^1$ bands.

To determine which charge carrier is trapped, the activation energy for the $^1S_0 \rightarrow {}^1I_6$ emission was determined using

$$I = C \exp \frac{\Delta E}{kT} \tag{1}$$

where I is the intensity, C is a constant, ΔE is a value for the activation energy, T the temperature (in K) and k is Boltzmann's constant.

A plot of $\ln I$ against $1/T$ and a least-squares fit to equation (1) are shown in figure 7. ΔE was found to be about 450 cm^{-1} (0.06 eV). This is a small value and we are therefore inclined to consider this energy as the de-trapping energy of a electron trap. It was found that the activation energy for migration of holes is typically of the order of tenths of electron volts [28]. Therefore it seems that the observation of the PCE process is caused by process (2). The activation energy of migration of STEs is about a factor of 2 or 3 smaller than the migration of V_K centres [29].

The different excitation, energy transfer and emission processes described above are illustrated in figure 8. The band gap of the $SrAlF_5$ materials is about 90 000 cm^{-1}, corresponding to 11 eV. Since $^1S_0$ emission was observed under x-ray excitation and under excitation into the lowest-energy $4f^15d^1$ band it is safe to assume that at least the lowest $4f^15d^1$ band is located below the conduction band edge of the material. As the energy difference between the $^3H_4$ and the lowest $4f^15d^1$ band is about 50 000 cm^{-1}, it can also be concluded that the $^3H_4$ ground state is located well above the top of the valence band. Pr^{3+} is then a stable hole trap. However, we do not know the relative position of the Pr^{3+} levels exactly with respect to the valence and conduction band. Just for illustration purposes, the Pr^{3+} energy levels are placed in the middle of the forbidden zone.

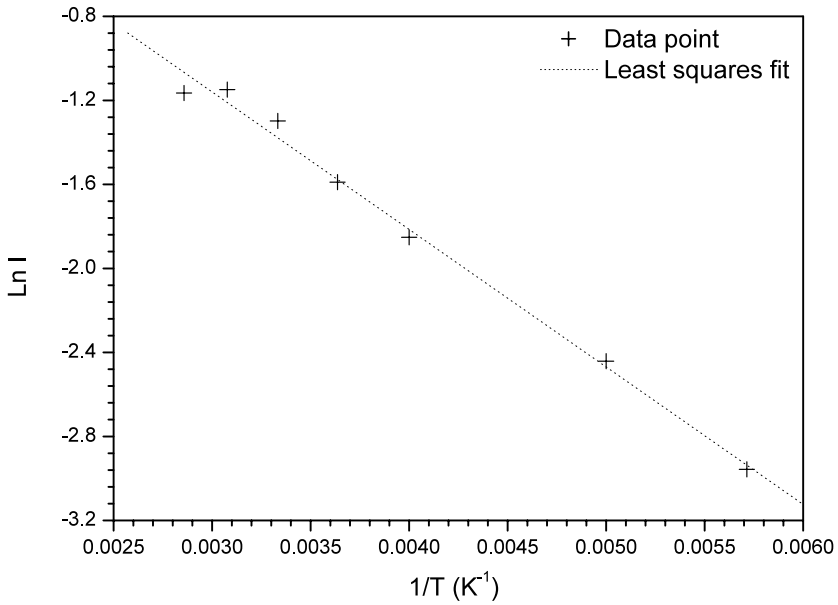

Figure 7. A $\ln I$ versus $1/T$ plot for the intensity of the $^1S_0 \rightarrow {}^1I_6$ transition ($\lambda_{em} = 404$ nm). The line is a least-squares fit to equation (1).

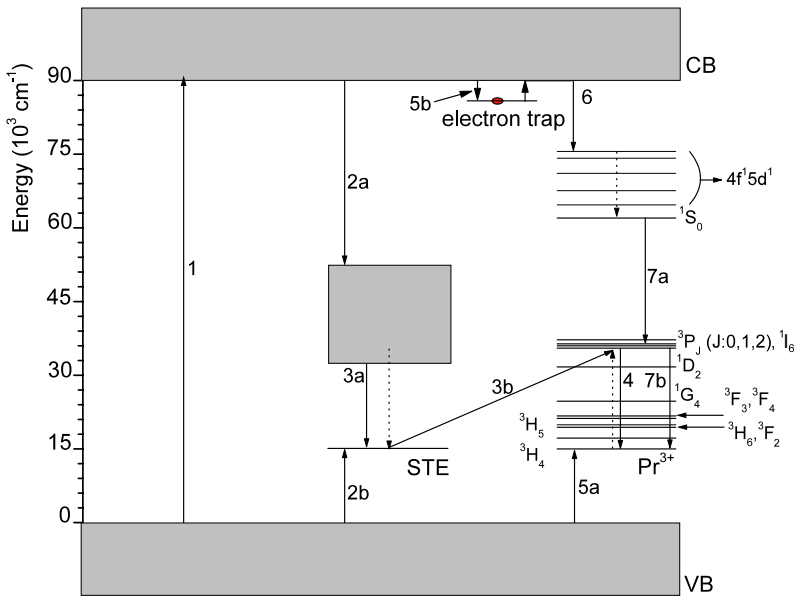

Figure 8. A schematic illustration of the different excitation, emission and energy transfer processes. The processes described in the text are numbered accordingly.
(This figure is in colour only in the electronic version)

The positions of the energy levels of the STE state compared to the valence and the conduction band are also not known. As there will be non-radiative energy transfer from the

STE to the Pr^{3+} levels, for illustration purposes the ground state of the STE and the Pr^{3+} $^3H_4$ ground state were chosen to be at the same position. From the temperature dependence of the $^1S_0$ emission it was found that the electron trap is at 450 cm^{-1}. We have drawn the trap level somewhat lower, at about 4 000 cm^{-1} below the bottom of the conduction band.

We can now summarize the different processes resulting in Pr^{3+} emission by using figure 8. Excitation of electrons into the conduction band results in holes in the valence band (step 1). The first process is the formation of a STE, which is shown as steps 2a and 2b. The STE can either emit radiatively (3a) or can transfer its energy to Pr^{3+} (3b). This energy transfer becomes more efficient at higher temperatures as the STE becomes mobile. Migration to Pr^{3+} is followed by energy transfer, populating the lower-lying (^3P_J, $^1I_6$ and $^1D_2$) Pr^{3+} levels. Emission from $^3P_0$ is shown as step 4.

The other process which leads to Pr^{3+} emission is the population of the lanthanide without an intermediate exciton state. Here, the hole is trapped on Pr^{3+} (step 5a) and the electron in an electron trap (5b). This situation does not result in any emission from praseodymium at temperatures lower than 150 K. Above this temperature, the electrons in the shallow traps are released and populate the higher $4f^15d^1$ bands of Pr^{3+} (step 6). This population of the $4f^15d^1$ bands results in two-photon emission, which is shown as $^1S_0 \rightarrow {}^1I_6$ (7a) and $^3P_0 \rightarrow {}^3H_4$ (7b) emission.

4. Conclusions

The optical properties of $SrAlF_5$:Pr^{3+} were studied. Under vacuum ultraviolet excitation in the $4f^15d^1$ bands this material shows the PCE process resulting in a number of different $^1S_0$, $^3P_0$ and $^1D_2$ emissions. When this material is excited with x-rays, the PCE process also occurs at high temperatures. Besides this process, STEs are formed, transferring energy, populating the Pr^{3+} ^3P_J ($J = 0, 1, 2$) and $^1I_6$ levels. This energy transfer is more efficient at higher temperatures. The PCE process in $SrAlF_5$:Pr^{3+} also proved to be temperature dependent. This is attributed to the electron in the conduction band, which is first trapped before it transfers its energy to Pr^{4+}.

The mechanism and energy transfer of $SrAlF_5$:Pr^{3+} under x-ray excitation, described in this paper, can probably also be found for Pr^{3+} in many different types of host.

Acknowledgments

The authors thank Dr M Kirm (HASYLAB, DESY Hamburg) for his assistance in the experiments performed on the SUPERLUMI set-up. The investigations described in this paper were supported by the Dutch Technology Foundation (STW) and by the IHP-Contract HPRI-CT-1999-00040 of the European Commission.

References

[1] Piper W W, de Luca J A and Ham F S 1974 *J. Lumin.* **8** 344
[2] Sommerdijk J L, Bril A and de Jager A W 1974 *J. Lumin.* **8** 341
[3] Wegh R T, Donker H, Oskam K D and Meijerink A 1999 *Science* **283** 663
[4] Wegh R T, van Loef E V D and Meijerink A 2000 *J. Lumin.* **90** 111
[5] van der Kolk E, Dorenbos P and van Eijk C W E 2001 *Opt. Commun.* **197** 317
[6] van der Kolk E, Dorenbos P, van Eijk C W E, Vink A P, Fouassier C and Guillen F 2002 *J. Lumin.* **97** 212
[7] Sokólska I and Kück S 2001 *Chem. Phys.* **270** 355
[8] Le Masson N J M, Vink A P, Dorenbos P, Bos A J J, Chaminade J P and van Eijk C W E 2002 *J. Lumin.* submitted

[9] Kück S and Sokólska I 2002 *J. Electrochem. Soc.* **149** J27
[10] Bayer E, Rossner W, Grabmaier B C, Alcalda R and Blasse G 1993 *Chem. Phys. Lett.* **216** 228
[11] Bayer E, Leppert J, Grabmaier B C and Blasse G 1995 *Appl. Phys.* A **61** 177
[12] Srivastava A M and Doughty D A 1996 *J. Electrochem. Soc.* **143** 4113
[13] Srivastava A M and Beers W W 1997 *J. Lumin.* **71** 285
[14] Srivastava A M and Doughty D A 1997 *J. Electrochem. Soc.* **144** L190
[15] van der Kolk E, Dorenbos P, Vink A P, Perego R C, van Eijk C W E and Lakshmanan A R 2001 *Phys. Rev.* B **64** 195129
[16] van der Kolk E, Dorenbos P and van Eijk C W E 2001 *J. Phys.: Condens. Matter* **13** 5471
[17] Weil M, Zobetz E, Werner F and Kubel F 2001 *Solid State Sci.* **3** 441
[18] Dubinskii M A, Schepler K L, Semashko V V, Abdulsabirov R Y, Korableva S L and Naumov A K 1998 *J. Mod. Opt.* **45** 221
[19] Rodnyi P A, Mikhrin S B, Dorenbos P, van der Kolk E, van Eijk C W E, Vink A P and Avanesov A G 2002 *Opt. Commun.* **204** 237
[20] Srivastava A M and Duclos S J 1997 *Chem. Phys. Lett.* **275** 453
[21] Schipper W J and Blasse G 1994 *J. Lumin.* **59** 377
[22] Zimmerer G 1991 *Nucl. Instrum. Methods Phys. Res.* A **308** 178
[23] Vink A P, van der Kolk E, Dorenbos P and van Eijk C W E 2002 *J. Alloys Compounds* **341** 338
[24] Dorenbos P 2000 *J. Lumin.* **91** 155
[25] Dorenbos P 2000 *J. Lumin.* **87–89** 970
[26] Van't Spijker J C, Dorenbos P, van Eijk C W E, Krämer K and Güdel H U 1999 *J. Lumin.* **85** 1
[27] Blasse G and Grabmaier B C 1994 *Luminescent Materials* (Berlin: Springer)
[28] Song K S 1971 *Solid State Commun.* **9** 1263
[29] Chen L F, Song K S and Leung C H 1990 *Nucl. Instrum. Methods Phys. Res.* B **46** 216